Design of a Compact 2 × 2 MIMO Diversity Antenna for X-band Applications

Tathababu Addepalli and V. R. Anitha

Abstract A compact 2 × 2 MIMO diversity antenna of size 32 × 32 × 1.6 mm^3 is presented in this paper for portable devices. The proposed structure uses polarization and pattern diversities for isolation enhancement. The orthogonal arrangement of radiating elements, pattern diversity, and defected ground structure is achieved isolation. The whole configuration is designed and fabricated over the FR4 substrate with ε_r 4.4, and fed by a 50Ω microstrip line. The proposed structure operates from 7.9 GHz to 13 GHz, and it resonates at 9 GHz, 12.3 GHz. The isolation between orthogonal elements is above 20 dB and the anti-parallel element is above 15 dB. The radiation efficiency and peak gain values are above 86% and 3.1–5.2 dB, respectively. The diversity metric value of ECC is less than 0.07, DG is above 9.985 dB, and TARC is below −10 dB for the entire desired band. Simulated and measured values are in good concord.

Keywords Multiple-input multiple-output (MIMO) · Isolation · Envelope correlation coefficient (ECC) · Diversity gain (DG) · Total active reflection coefficient (TARC) · X-band applications

1 Introduction

Nowadays, wireless communication technologies are increasing rapidly because of various applications like cordless telephones, satellite television, GPS, WIFI, WLAN, WiMAX, and wireless computer parts, but they require high data rate transmission and reliability. Using the MIMO technology can achieve the above requirements with multiple radio channels placed on the transmitting end and the receiving end. But it

T. Addepalli (✉)
Department of ECE, JNTUA, Ananthapur, Andra Pradesh, India
e-mail: babu.478@gmail.com

V. R. Anitha
Antenna Research Laboratory, Sree Vidyanikethan Engineering College, Tirupathi, Andra Pradesh, India
e-mail: anithavr@ieee.org

does not require additional bandwidth and input power. In portable devices, antennas are placed very closely. Due to the limited space between the antennas, the radiation from individual antennas collides with each other. Hence, the receiving end can't receive the original information due to coupling. This also leads to degrading system performance and channel capacity. So the coupling between antennas becomes a major problem in the MIMO technology.

Coupling arises due to the collision of radiation from antennas in free space, the current flowing on the metals, and surface waves in the dielectric substrate [1]. The effect of coupling between antennas in the same substrate can't be minimized easily due to the compactness. It degrades system performance and SNR value [2]. Different techniques are there for the reduction of mutual coupling like pattern diversity and polarization diversity, by changing the orientation of the antenna and placing decoupling networks between the antennas. The polarization diversity is achieved through the orthogonal arrangement of antenna elements with different polarization, where one is horizontal and the other one is a vertically polarized antenna. The following literature describes the four antenna elements that are arranged in rows and columns in isolation enhancement, and the size of the MIMO structure is also specified.

The arrangement of four radiating elements on a common substrate with low mutual coupling is a challenging issue for the MIMO design. The polarization diversity of a MIMO antenna with size 270×210 mm^2 and the isolation improvement is 20 dB [3]. Antenna elements are arranged in an orthogonal manner with isolation; they even have the same radiation patterns [4]. The size of the conical-shaped array antenna was 200×200 mm^2 with an isolation of 20 dB [5]. A new wideband slot array with polarization diversity (size = 114×114 mm^2) results in an isolation improvement of higher than 25 dB [6]. The substrate of size 100×120 mm^2 consists of four dipole antennas that are placed in an orthogonal manner for isolation enhancement and also to achieve multi-beam radiation patterns [7]. An inset-fed four-element rectangular-shaped MIMO antenna of size 100×50 mm^2 is designed for ISM band applications, and the isolation of 10 dB is achieved using CSRR structure [8]. The substrate of size 95×60 mm^2 consisting of four radiating elements is placed in its corners for isolation enhancement (S21 < 11.5 dB) [9]. Similarly, four-slot antennas are arranged on the substrate of size 70.11×70.11 mm^2 in an orthogonal manner for isolation [10]. A G-shaped MIMO antenna with an isolation of 21 dB using polarization diversity of size 70×70 mm^2 [11]. The G-shaped antenna elements are arranged in a parallel manner in the MIMO structure of size 55×50 mm^2 is designed for wireless portable applications and the L-shaped stubs with inverted T-shaped slot are used for the isolation enhancement [12]. Four inverted L-shaped antennas with a rectangular-shaped CSRR structure for isolation enhancement better than 17 dB are used and also low ECC values are achieved [13]. A diamond-shaped patch with four orthogonal feeds of structure size 120×140 mm^2 is used and the isolation achieved is better than 15 dB with a ground plane cutting in proper place [14].

Most of the work in the literature is about four-element antennas, which are arranged in an orthogonal manner for isolation and are also larger in size and so it is difficult to design the structures. But, the proposed structure is of compact nature and easy to design. Four antenna elements are arranged in an orthogonal manner

for better isolation of structure size 32×32 mm^2 and fabricated on FR4 dielectric material with a dielectric constant 4.4. It covers the entire X-band applications, i.e., 7.9–13 GHz. Orthogonal elements in the structure give an isolation of more than 20 dB and the anti-parallel elements give an isolation of above 15 dB.

2 Antenna Design Procedure

The proposed structure, a compact 2×2 MIMO antenna, is shown in Fig. 1a–d. The overall structure size is $32 \times 32 \times 1.6$ mm^3. It is simulated and fabricated on a low-cost FR4 substrate material of height 1.6 mm with dielectric constant (€r) 4.4. The shape of the top layer of the proposed structure is three half circles cutting (left, right, and top) the circular patch antenna with inside feed, and the shape of the bottom layer of the proposed antenna has defected ground structure with small
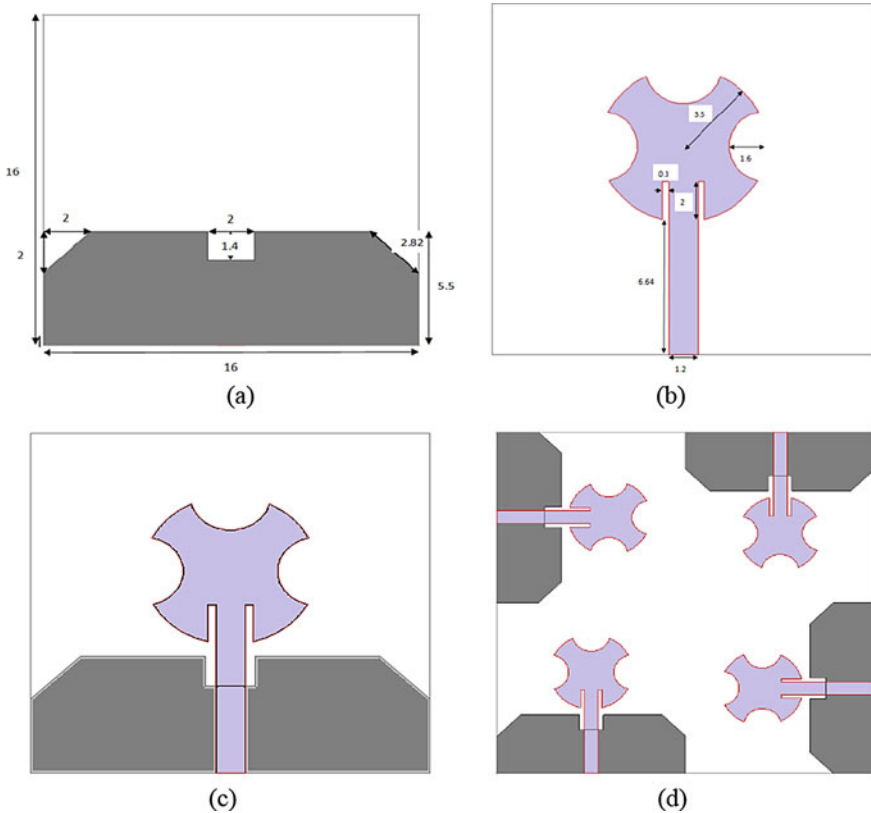

Fig. 1 a and **b** Geometry of bottom and top layers; **c** Proposed single-element antenna; **d** Proposed 2 × 2 MIMO structure

rectangular slit and edge cuttings. The proposed structure bottom layer is formed by a small triangular-shaped patch is removed at both edges of the partial ground plane, and a small rectangular-shaped patch removed in the centre of the partial ground plane. The photographs of the fabricated proposed structure top and bottom layers are shown in Fig. 2a, b. The design and evolution procedure of the proposed structure is shown in Fig. 3a–f.
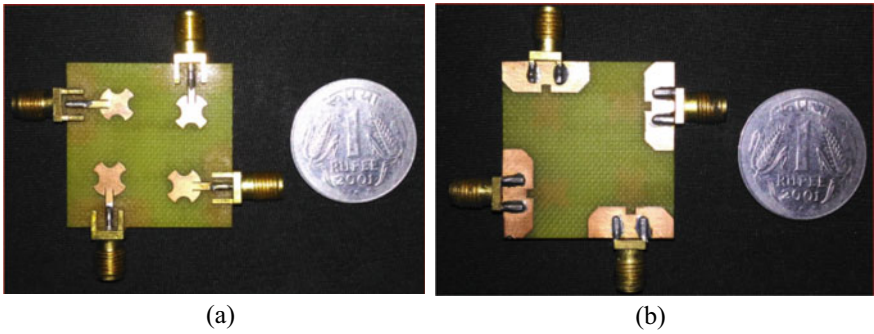

(a)   (b)

Fig. 2 **a** and **b** are photographs of fabricated proposed structure top and bottom layers

(a)   (b)   (c)

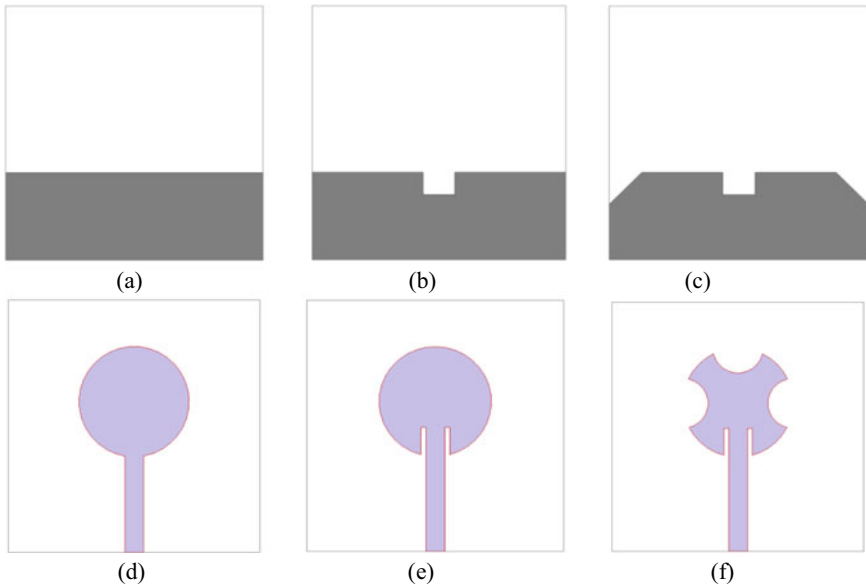(d)   (e)   (f)

Fig. 3 Design process of proposed structure

3   Simulation and Measurement Results

Figure 4 shows the design procedure of the proposed structure. For getting the desired results, the optimization process is also done. The simulated results of three antenna configurations with the proposed 2 × 2 MIMO structure are shown in Fig. 5a. From the figure, it is observed that the variation in the bandwidth of the proposed single element and 2 × 2 MIMO structure is slightly varying. It is due to the coupling between the orthogonal elements and anti-parallel elements. However, the proposed 2 × 2 structure covers the complete X-band application and also achieves better isolation.

S-parameters are the most important parameters for any antenna design. The reflection coefficient (S11) is "the ratio of the reflected to the incident power", but return loss is the dB's representation of the reflection coefficient. The transmission coefficient (S21) describes the total transmitted power relative to the incident power. The acceptable value of the transmission coefficient of theMIMO design is minimum −15 dB. Figure 5a, b shows the S-parameter comparison of antenna configuration and comparison of simulated and measured S-parameter values when port 1 is excited, respectively. The simulation and measurement values of the proposed structure are slightly varied. In simulation results, the lower band starts at 7.9 GHz but in measured results, the lower band starts at 8.3 GHz; this is due to tolerances at the inside feed cutting and soldering problems. Figure 5c, d shows the photographs of S11- and S21-parametrs of Anritsu MS2073C VNA (vector network analyzer) master.

Figure 6a–d illustrates the comparison of isolation when individual ports are excited. For adjacent radiating elements, the isolation is above 20 dB and the isolation is above 15 dB for diagonal radiating elements. The reason is adjacent elements are orthogonal to each other and due to this, one is a horizontally polarized antenna and the other one is a vertically polarized antenna. Diagonal elements are in the same polarization, but are in the opposite direction. Hence, the orthogonal elements have more isolation compared to the diagonal elements.

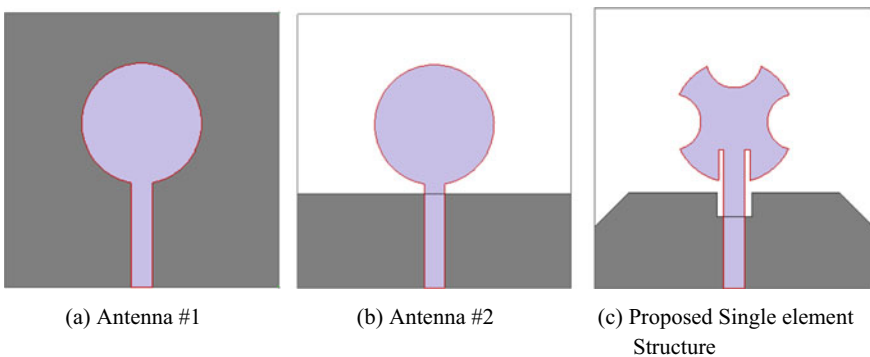Figure 7 shows the peak gain and radiation efficiency of the proposed 2 × 2

(a) Antenna #1   (b) Antenna #2   (c) Proposed Single element
                                                        Structure

Fig. 4 **a**, **b**, and **c** the design process of three antenna configuration

(a)

(b)

(c)   (d)

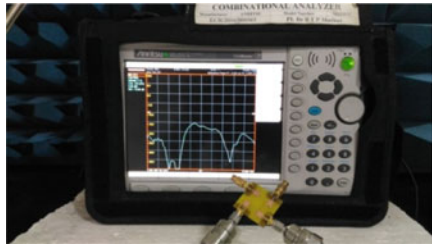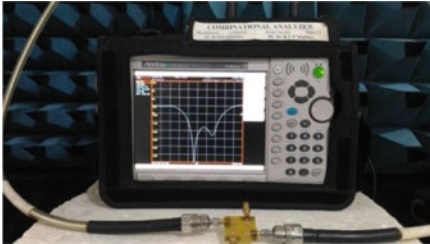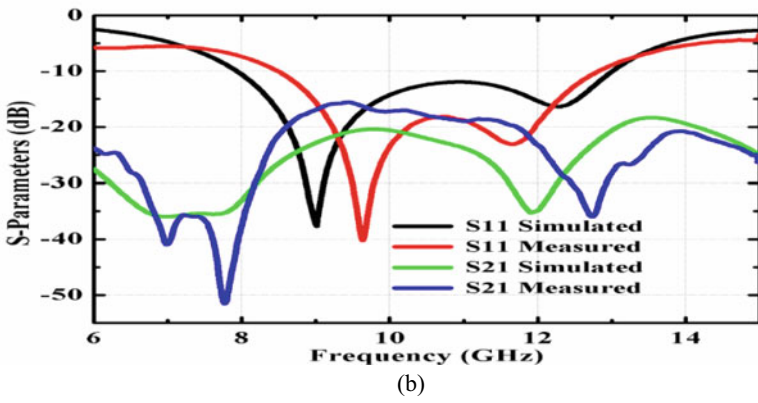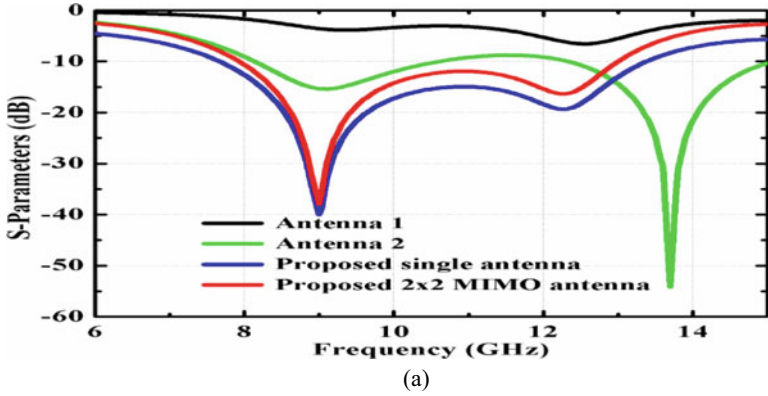**Fig. 5** **a** S11 values of three antenna configuration with proposed 2 × 2 MIMO; **b** measured and simulated values of 2 × 2 MIMO proposed structures; **c** and **d** are photographs of measured S11 and S21 values
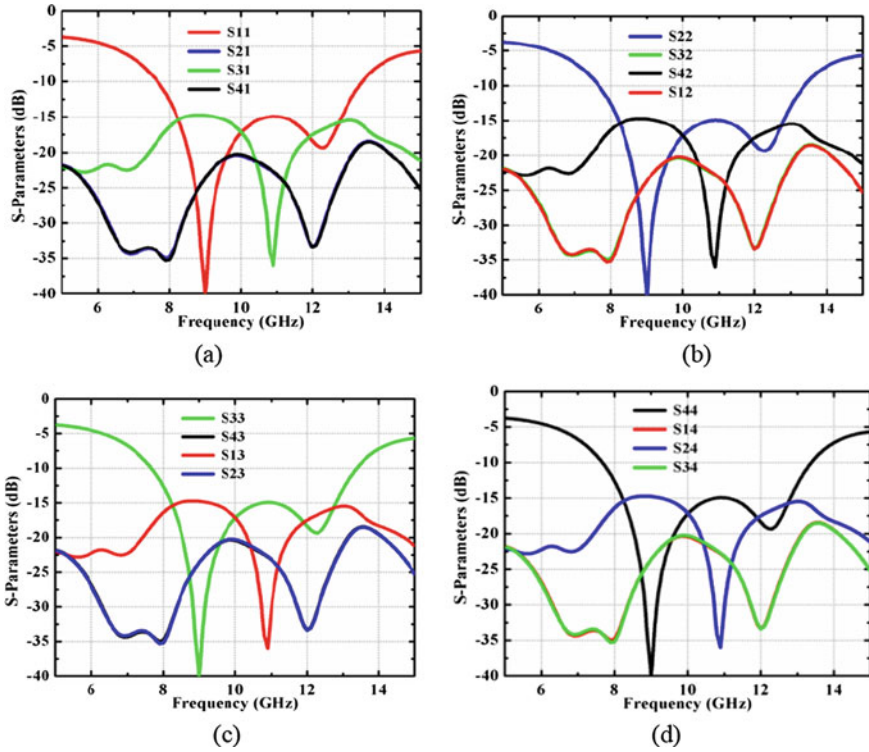
Fig. 6 a Simulated S-parameters of proposed structure when port 1 is excited; **b** Simulated S-parameters of proposed structure when port 2 is excited; **c** Simulated S-parameters of proposed structure when port 3 is excited, and **d** Simulated S-parameters of proposed structure when port 4 is excited
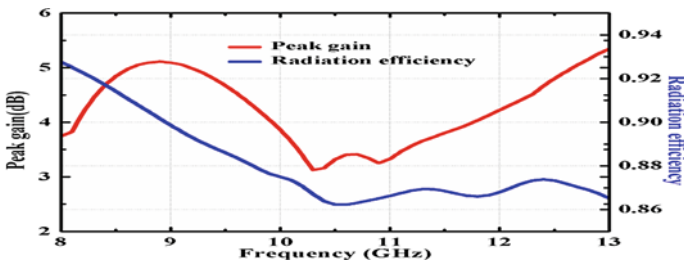

Fig. 7 Simulated peak gain and radiation efficiency results

MIMO structure having a peak gain of 5.09 dB at 9 GHz and 4.50 dB at 12.3 GHz and having more than 86% for the entire band, respectively.

Figure 8a, b shows the surface current distribution of the proposed 2 × 2 MIMO structure at 9 GHz and 12.3 GHz resonant frequencies. It is one of the observation

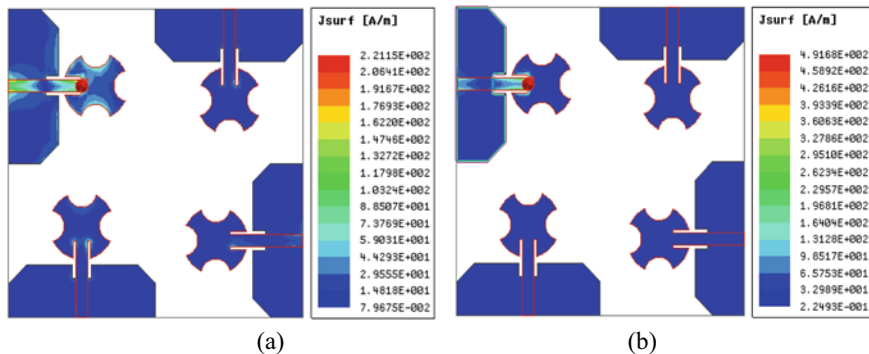(a)   (b)

Fig. 8 **a** Surface current distribution at 9 GHz when port 1 is excited; **b** Surface current distribution at 12.3 GHz when port 1 is excited

parameters in the MIMO design for observing the effect of one antenna on the other antenna and is also useful for observing the flow of current on the metals. By observing the surface current distribution on the metal, it will be decided which part of the radiating element is more excited, and based on that the shape of the antenna will be changed to the user requirement. Figure 9 describes the pattern diversity performance of the proposed structure. Figure 10 describes the polarization diversity of the proposed structure. The study of the time-varying electrical behavior of an electric field (E-field) is known as polarization.

Figure 11a, b describes the simulation 2D radiation patterns of the proposed 2 × 2 MIMO structure when port 1 is excited and the remaining three ports are with 50Ω termination loads.

MIMO Performance

ECC is useful to estimate the diversity performance of the MIMO antenna and also determines the similarities between the radiation patterns [15]. The proposed structure ECC value is computed from S-parameter values using the equation given by Blench et al. [16] represented in Eq. (1). The relation between ECC and DG is in Eq. (2).

$$ECC = \frac{\left| S_{11}^* \, S_{12} \; + \; S_{21}^* \, S_{22} \right|^2}{\left(1 - |S_{11}|^2 \; - \; |S_{21}|^2 \right) \left(1 - |S_{22}|^2 \; - \; |S_{12}|^2 \right)} \tag{1}$$

$$DG = 10\sqrt{1 - ECC^2} \tag{2}$$

The low value of ECC defines that there is less overlapping between the radiating elements. The acceptable value of the MIMO design is below 0.5. Figure 12a describes the simulation values of ECC and DG, which are lower than 0.07 and above 9.985, respectively. In MIMO antennas, S-parameter values of individual elements will not give the overall system performance correctly. Because it considers only
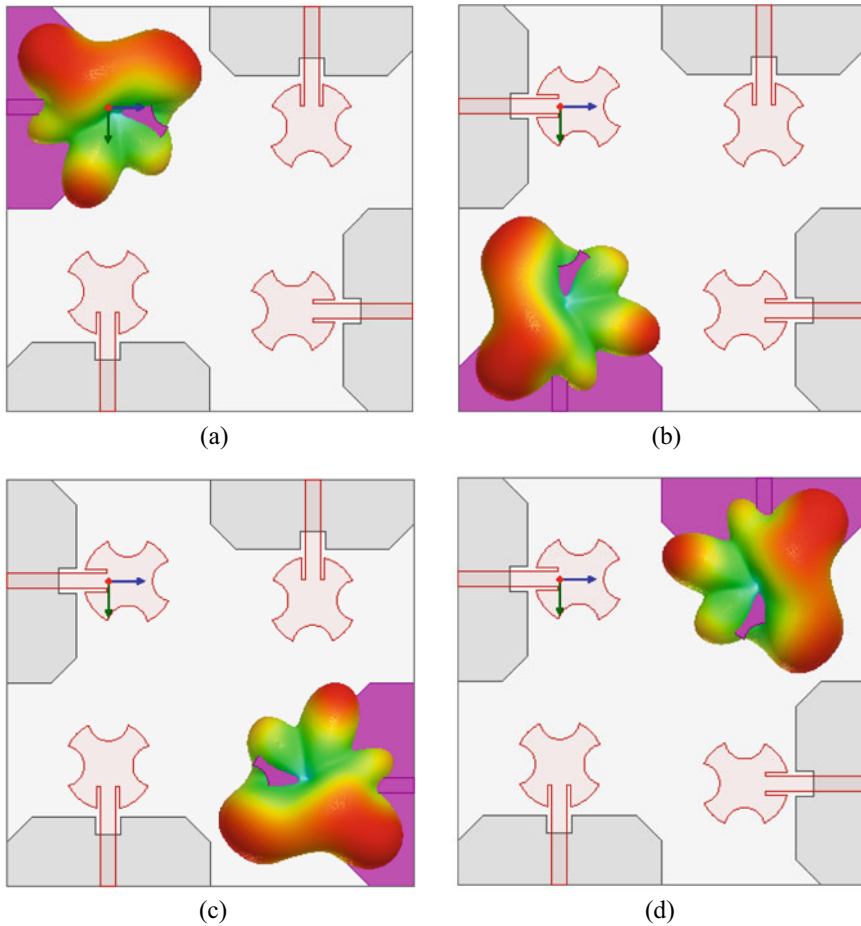
(a)   (b)

(c)   (d)

Fig. 9 **a** Radiation pattern at port 1; **b** Radiation pattern at port 2; **c** Radiation pattern at port 3; **d** Radiation pattern at port 4

the characteristic impedance of the individual antenna elements, but not mutual impedances. Changes in the self- and mutual impedances due to the adjacent antenna will not be considered. Hence, the term TARC is required for analyzing system performance in an accurate way. TARC is represented in terms of S-parameters and it is represented in Eq. (3). Figure 12b shows the comparison of S-parameters with TARC values. TARC values are calculated between orthogonal elements in the proposed structure. The acceptable values in the MIMO antenna design are <0 dB.

$$TARC = \sqrt{\frac{(S_{11} + S_{12})^2 + (S_{21} + S_{22})^2}{2}} \qquad (3)$$
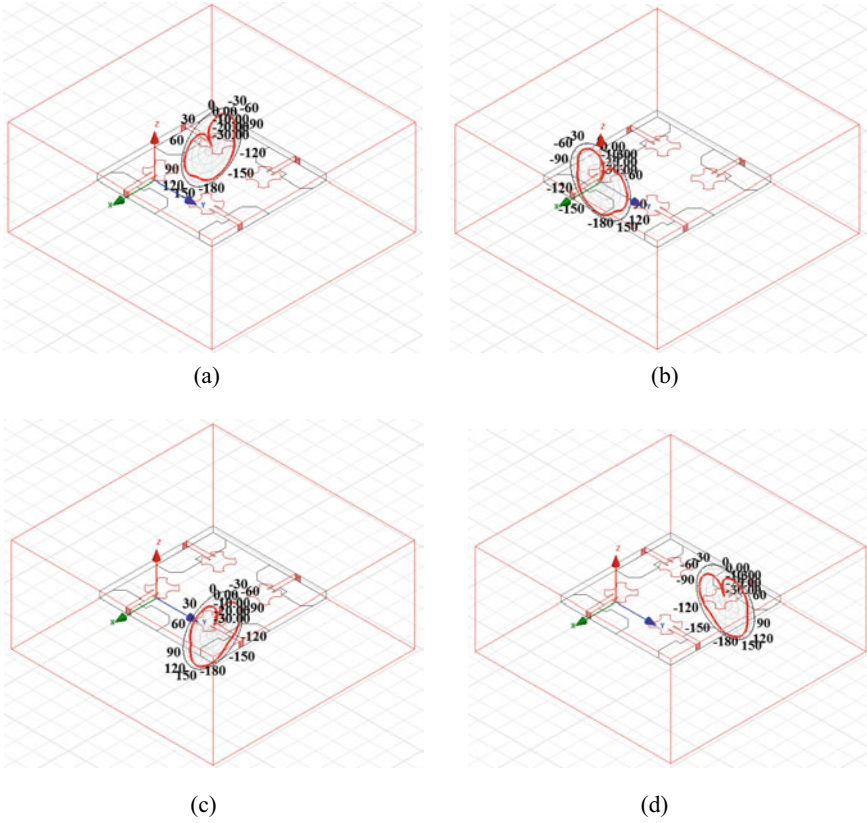
(a)   (b)

(c)   (d)

Fig. 10 a E-field at port 1 (on XZ-plane); **b** E-field at port 2 (on YZ-plane); **c** E-field at port 3 (on XZ-plane); **d** E-field at port 4 (on YZ-plane)

4 Conclusion

A compact 2×2 MIMO diversity antenna is presented in this paper. It is operated in the X-band region, i.e., from 7.9 GHz to 13 GHz and resonates at 9 GHz and 12.3 GHz. The simulation and measurement of S-Parameter values are presented. The isolation between adjacent elements is above 20 dB and between diagonal elements it is above 15 dB. Low ECC, high DG, and acceptable TARC values are achieved. The peak gain and antenna efficiency are also presented for X-band portable device applications.
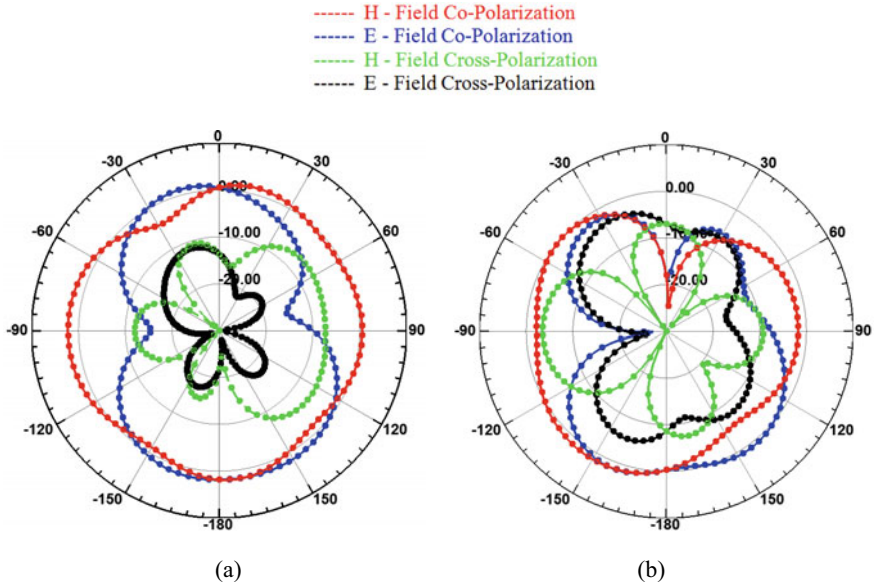
------ H - Field Co-Polarization
------ E - Field Co-Polarization
------ H - Field Cross-Polarization
------ E - Field Cross-Polarization

(a)   (b)

Fig. 11 a E (Co and Cross) and H (Co and Cross) fields at 9 GHz when port 1 is excited; **b** E (Co and Cross) and H (Co and Cross) fields at 12.3 GHz when port 1 is excited
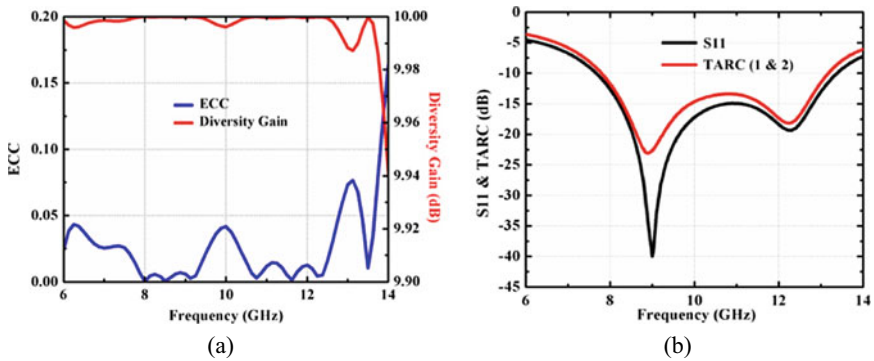

(a)   (b)

Fig. 12 a Simulated ECC and DG results; **b** Simulated S11 and TARC results

References

1. Chen X, Zhang S, Li Q (2018) A review of mutual coupling in MIMO systems. IEEE Access, April 2018. https://doi.org/10.1109/ACCESS.2018.2830653
2. Yuan Q, Chen Q, Sawaya K (2006) Performance of adaptive array antenna with arbitrary geometry in the presence of mutual coupling. IEEE Trans Antennas Propag 54(7):1991–1996, Jul 2006. https://doi.org/10.1109/TAP.2006.877158

3. Yeap SB, Chen X, Dupuy JA, Chiau CC, Parini CG (2005) Integrated diversity antenna for laptop and PDA terminal in a MIMO system. IEE Proc, Microw Antennas Propag 152(6):495–504. https://doi.org/10.1049/ip-map:20045062

4. Li H, Xiong J, He S (2009) A compact planar MIMO antenna system of four elements with similar radiation characteristics and isolation structure. IEEE Antennas Wirel Propag Lett 8:1107–1110. https://doi.org/10.1109/LAWP.2009.2034110

5. Sim CYD (2012) Conical beam array antenna with polarization diversity. IEEE Trans Antennas Propag 60(10):4568–4572. https://doi.org/10.1109/TAP.2012.2207319

6. Costa JR, Lima EB, Medeiros CR, Fernandes CA (2011) Evaluation of a new wideband slot array for MIMO performance enhancement in indoor WLANs. IEEE Trans Antennas Propag 59(84):1200–1206. https://doi.org/10.1109/TAP.2011.2109685

7. Chang DC, Zeng BH, Liu JC (2009) Reconfigurable angular diversity antenna with quad corner reflector arrays for 2.4 GHz applications. IET Microw Antennas Propag 3(37):522–528. https://doi.org/10.1049/iet-map.2008.0119

8. Sharawi MS, Khan MU, Numan AB, Aloi DN (2013) A CSRR loaded MIMO antenna system for ISM band operation. IEEE Trans Antennas Propag 61(8):4265–4274. https://doi.org/10.1109/TAP.2013.2263214

9. Ding Y, Du Z, Gong K, Feng Z (2007) A four element antenna system for mobile phones. IEEE Antennas Wirel Propag Lett 6:655–658. https://doi.org/10.1109/LAWP.2007.913276

10. Zhang S, Zetterberg P, He S (2010) Printed MIMO antenna system of four closely spaced elements with large bandwidth and isolation. Electron Lett 46(15):1052–1053. https://doi.org/10.1049/el.2010.1445

11. Malviya L, Panigrahi RK, Kartikeyan MV (2016) A 2×2 dual band MIMO antenna with polarization diversity for wireless applications. Progr Electromagn Res C 61:91–103

12. Xia XX, Chu Q-X, Li JF (2013) Design of a compact wideband MIMO antenna for mobile terminals. Progr Electromagn Res C 41: 163–174, July 2013

13. Ntaikos DK, Yioultsis TV (2013) Compact split ring resonator loaded multiple input multiple output antenna with electrically small elements and reduced mutual coupling. IET Microw Antennas Propag 7(6):421–429. https://doi.org/10.1049/iet-map.2012.0688

14. Moradikorordalivand A, Rahman TA, Khalily M (2014) Common elements wideband MIMO antenna system for WiFi/LTE access point applications. IEEE Antennas Wirel Propag Lett 13:1601–1604. https://doi.org/10.1109/LAWP.2014.2347897

15. Rao Jetti C, Nandanavanam VR (2018) Trident-shape strip loaded dual band-notched UWB-MIMO antenna for portable device applications. ELSEVIER, Int J Electron Commun (AEÜ) 83:11–21. https://doi.org/10.1016/j.aeue.2017.08.021

16. Blanch S, Romeu J, Corbella I (2003) Exact representation of antenna system diversity performance from input parameter description. Electron Lett 39 (9):705–707. https://doi.org/10.1049/e1:200304Y5